Journal of Russian Laser Research, Volume 29, Number 3, 2008

ATOM IN ELECTROMAGNETIC FIELD OF NEAR-ATOMIC STRENGTH*

A. V. Andreev, S. Yu. Stremoukhov, and O. A. Shoutova

Faculty of Physics and International Laser Center
M. V. Lomonosov Moscow State University
Vorob'evy Gory, Moscow 119992, Russia
e-mails: av_andreev@phys.msu.ru sustrem@gmail.com olya.shoutova@gmail.com

Abstract

Ionization and high-harmonics generation in a single hydrogen-like atom driven by a laser pulse of near-atomic field strength is the subject of this paper. We use exact solutions of the eigenvalue problem on particle motion in the cylindrically symmetric field (CSF) as a basis for the wave-function expansion. The superposition of the spherically symmetric intra-atomic field and linearly polarized laser field has the cylindrical symmetry. Hence, the use of the free-atom eigenfunctions as a basis for the wave-function expansion requires an infinitely increasing number of spherical harmonics (i.e., free-atom eigenfunctions) when the laser field strength approaches the intra-atomic field value. The eigenfunctions of the CSF problem depend on the laser field strength; therefore, the appropriate matrix elements show how the spectral width of atomic response and angular selection rules vary with increase in the laser field strength. The introduction gives a phenomenological semiclassical illustration of the problem.

Keywords: atom in e.m. field, ionization, selection rules, high-harmonics generation, cutoff frequency, laser fields of near-atomic strength, Schrödinger equation.

1. Introduction

The effect of high optical harmonic generation (HHG) with or without ionization is one type of nonlinear atomic response to a strong laser field. The physical mechanisms of this effect are under active investigation since the discovery of above-threshold ionization (ATI) by Agostini with coauthors in 1979, when according to Becker's review "intense-laser atom physics entered the non-perturbed regime" [1]. The following general features can characterize the emission spectra of atoms driven by the laser field. The laser field induces a time-varying dipole moment $\vec{d}(t)$. At a low intensity of the laser pulse, the frequency of induced dipole-moment variations is exactly determined by the laser pulse carrier frequency: $\vec{d}(t) \sim \exp(-i\omega t)$. The increase in the laser-field intensity results in the appearance of odd harmonics of the laser frequency. Even harmonics are forbidden due to the space inversion symmetry of the intra-atomic field $U(\vec{r}) = U(-\vec{r})$. The amplitude of the nth harmonic is proportional to $\left(\vec{d}\vec{E}/\hbar\omega\right)^n$, where $\vec{d}\vec{E}$ is the energy of electro-dipole interaction and $\hbar\omega_0$ is the mean energy of atomic transitions. Under

*Talk presented at the oral issue of J. Russ. Laser Res. dedicated to the memory of Professor Vladimir A. Isakov, Professor Alexander S. Shumovsky, and Professor Andrei V. Vinogradov held in Moscow February 21–22, 2008.

Manuscript submitted by the authors in English on April 16, 2008.
1071-2836/08/2903-0203

a further increase in the laser-pulse intensity, the spectrum of response takes the form of a plateau, i.e., a sequence of odd harmonics with approximately equal amplitudes and sharp cut-off frequency. In the subatomic region of the laser field strength $E \ll E_{at}$, the cut-off frequency depends linearly on the laser-pulse intensity.

An overwhelming number of theoretical approaches have been developed to explain such behavior of atomic emission spectra in dependence on the laser-field intensity. We use the Bohr model of the atom to illustrate the basic physics of the process of atomic response. The classical equation for an electron interacting with the intra-atomic and laser fields is

$$m\ddot{\vec{r}} = -\frac{\partial U}{\partial \vec{r}} + e\vec{E}. \tag{1}$$

In the case of a free atom, the scalar product of this equation with $\dot{\vec{r}}$ and the vector product with $\vec{r}$ yield the energy and angular-momentum conservation laws

$$\frac{d}{dt}\left(\frac{m\dot{\vec{r}}^2}{2} + U(r)\right) = 0, \qquad \frac{d}{dt}\left(m\left[\vec{r}\dot{\vec{r}}\right]\right) = 0. \tag{2}$$

According to the Bohr quantization rules, for the ground atomic state we have

$$m\rho^2\dot{\varphi} = \hbar, \tag{3}$$

where we have assumed that the electron makes a motion in the plane $z = 0$. By substituting (3) into the energy conservation law, we obtain

$$\frac{d}{dt}\left(\frac{\hbar^2}{2m\rho^2} - \frac{e^2}{\rho}\right) = 0.$$

Hence, the radius of the orbit of the steady-state motion (when $\dot{z} = 0$ and $\dot{\rho} = 0$) is

$$\rho_0 = \frac{\hbar^2}{me^2} = a_B,$$

where a_B is the Bohr radius. The state energy equals to

$$\varepsilon_0 = \frac{\hbar^2}{2m\rho_0^2} - \frac{e^2}{\rho_0} = -\frac{me^4}{2\hbar^2} = -\frac{Ry}{2}.$$

The latter coincides with the energy of the ground state of the hydrogen atom.

Let now the atom interact with the linearly polarized wave. In this case, we have the following equation for angular momentum:

$$\frac{d}{dt}\left(m\left[\vec{r}\dot{\vec{r}}\right]\right) = e\left[\vec{r}\vec{E}\right]. \tag{4}$$

It is seen that the projection of angular momentum on the electric-field direction is still the integral of motion. Hence, if the laser-field polarization coincides with the z axis, then the electron, performing free motion in the plane $z = 0$, starts to make the quiver motion perpendicular to this plane. In a weak laser field, a quiver-motion amplitude is very small, $a_0 \ll a_B$, hence the Coulomb field does not affect the electron quiver motion, because

$$r(t) = \sqrt{\rho_0^2 + z^2(t)} \approx \rho_0.$$

In this case, the z component of the electron velocity is

$$\dot{z}_0 = -eA\,(t)/mc,$$

where $A\,(t)$ is the vector potential of the laser field. The spectrum of atomic response is given by the velocity Fourier transform. It is seen that when the quiver-motion amplitude $a_0 = eE_0/m\omega^2$ satisfies the condition $a_0 \ll a_B$, the spectrum of response is strongly dominated by the laser carrier frequency. Notice that the last condition can be rewritten as $ea_BE_0 \ll \hbar^2\omega^2/Ry \approx \hbar\omega$. If the laser field does not coincide with the direction of orbital angular momentum, the orbital momentum precesses around the laser-field direction.

With increase in the laser-field amplitude E_0, the difference $\sqrt{\rho_0^2 + z^2} - \rho_0$ may take an appreciable value. Let us introduce the deviation $\delta z = z\,(t) - z_0\,(t)$. The scalar product of Eq. (1) with $\dot{\vec{r}} + e\vec{A}/mc$ yields the following energy-conservation law:

$$\frac{d}{dt}\left[\frac{1}{2m}\left(m\dot{\vec{r}} + \frac{e}{c}\vec{A}\right)^2 + U\,(x, y, z_0 + \delta z)\right] = 0. \tag{5}$$

If the deviation is small $|\delta z| < a_0$, we arrive at

$$\dot{z} = \dot{z}_0 + \sqrt{\frac{e^2}{m}\left(\frac{1}{\rho_0} - \frac{1}{\sqrt{\rho_0^2 + z_0^2\,(t)}}\right)} = \dot{z}_0 + \frac{e^2}{\hbar}\sqrt{1 - \frac{1}{\sqrt{1 + (z_0\,(t)\,a_B)^2}}}. \tag{6}$$

At $z_0 < a_B$, the last equation converts into

$$\dot{z} = \dot{z}_0 + z_0\,(t)\,\frac{e^2}{\hbar a_B}\sqrt{\sum_{n=0}^{\infty}(-1)^n\,\frac{\Gamma\,(n + 3/2)}{\Gamma\,(1/2)\,\Gamma\,(n + 2)}\left(\frac{z_0\,(t)}{a_B}\right)^{2n}}.$$

It is seen that at $a_0 \ll a_B$ the emission spectrum of the atom interacting with the monochromatic laser field $E = E_0 \cos\omega t$ is a sequence of odd harmonics with amplitudes proportional to $(a_0/a_B)^{2n+1}$. Notice that, according to the binomial theorem, we have for $(z_0\,(t)/a_B)^{2n}$

$$\cos^{2n}\omega t = \sum_{m=0}^{2n} C_{2n}^m \exp\left[i2\omega\,(n - m)\,t\right].$$

As a result, the amplitude of the $(2k + 1)\,\omega$ harmonic is the infinite sum of n at $m = n - k$. Hence, the profile of the atomic response spectrum will inevitably undergo transformations if the amplitude of electron oscillations a_0 approaches a_B.

In a very strong laser field, the distance between electron and nucleus can exceed the Bohr radius at some time moments. It is seen from Eq. (6) that at these time moments $\dot{z} \approx \dot{z}_0$, hence, the amplitudes of the harmonics are drastically suppressed. So, it becomes evident that the spectrum of response saturates when $a_0 > a_B$. Indeed, the saturation of the cut-off frequency with increase in the laser-pulse intensity has been demonstrated in recent experiments by Ganeev et al. [7].

In the above consideration, we have assumed that the intra-atomic potential is the Coulomb field potential. As it is clearly seen from the right-hand side of Eq. (6), the profile of atomic response depends

drastically on the spatial profile of the intra-atomic potential. For example, the spectrum of response will not include harmonics if we assume that $U(r) = Cr^2$. Hence, the spectrum of the heavy atom response may differ from that for the hydrogen atom because the nucleus shielding effect becomes important for heavy atoms. In deriving Eq. (6), we have assumed that the electron motion in the plane $z = 0$ remains invariable. Thus, Eq. (6) demonstrates clearly that the nature of the HHG effect should not be directly associated with the electron transitions between the different atomic steady states. At the same time, the electron internal motion remains invariable only in the case where the laser field is directed perpendicular to the plane of internal electron motion. In the general case, we should analyze the coupled set of equations (4) and (5). The difference between these two processes can be easily understood without exact solving of these equations. Indeed, it is clearly seen from Eq. (5) that, if we take into account transitions between the atomic steady states, then, in general, the emission spectra may include harmonics even in the harmonic potential well, i.e., $U(r) = Cr^2$. However, the amplitude of the harmonics will be very small. Thus, the origin of the nonlinear atomic response is quite reasonably modeled by Eq. (6), which demonstrates clearly the main mechanisms of this process and provides fundamentals of the physics.

The classical theory can work only as a qualitative model of the phenomenon, because it does not provide a consistent description of the electron transitions between the atomic steady states. A consistent theory should be based on the use of the wave equations.

We are interested in the specific features of the atomic emission spectra and angular distributions of ionized electrons in the case where the laser-field strength approaches the atomic-field strength. The above discussion shows clearly that, in this region of the laser field strength, the precise calculations could not be based on the perturbation methods, which rely on the smallness of the ratio of the laser-field strength to the intra-atomic-field strength. Several non-perturbed schemes have been developed for modeling the emission spectra of atoms driven by high-intensity laser fields; for example, methods employing the Floquet theory [6], dressed states [5], classical trajectories [4], and direct numerical integration of the time-dependent Schrödinger equation [3]. Our method falls within the framework of these studies and deals with exact solutions of the eigenvalue problem for electron motion in a cylindrically symmetric external field [2].

This paper is organized as follows.

Section 2 gives a further development of the approach proposed in [2,9,10]. Section 3 is devoted to analytical and numerical calculations of photoemission spectra. In Sec. 4, we represent angular distributions of ionized electrons.

2. Basic Relations and Foundation of the Method

The Schrödinger equation for an atom interacting with an external electromagnetic field has the form

$$i\hbar\frac{\partial\psi}{\partial t} = \left[\frac{1}{2m}\left(\vec{p} - \frac{q}{c}\vec{A}\right)^2 + U\right]\psi, \tag{7}$$

where $U(\vec{r})$ is the intra-atomic-field potential energy and $\vec{A}(t)$ is the vector potential of the external electromagnetic field. The standard algorithm for its solution consists in the wave function expanding into a series of free-atom eigenfunctions

$$\psi = \sum_{n,l} a_{n,l}(t) u_{n,l}(\vec{r}) + \int dk\; a(k,l,t)\, u(k,l,\vec{r}) \tag{8}$$

and decomposition of the Hamiltonian of Eq. (7) into a sum of the free-atom Hamiltonian H_0 and the interaction Hamiltonian H_{int}

$$H_0 = \frac{\vec{p}^2}{2m} + U, \qquad H_{\text{int}} = -\frac{q}{2mc}\left(\vec{p}\vec{A} + \vec{A}\vec{p}\right) + \frac{q^2}{2mc^2}\vec{A}^2.$$

In comparatively weak fields, the matrix elements of the interaction Hamiltonian are much smaller than the matrix elements of the free-atom Hamiltonian. In this case, series (8) includes a relatively small number of significant terms. However, the symmetry of the problem (7) differs from the spherical symmetry of the free-atom problem. Hence, the increase in the laser-pulse intensity results in an infinite increase in the number of significant terms in series (8), because the spherical harmonics are not eigenfunctions of the general problem (7).

Let us consider now the Hamiltonian of Eq. (7). It is possible to establish the relationships between the eigenvalues and eigenfunctions of this Hamiltonian and the free-atom Hamiltonian in a general mathematical form. Indeed, let $u_n(\vec{r})$ be the complete set of eigenfunctions for the free-atom boundary value problem

$$\left(\frac{p^2}{2m} + U(\vec{r})\right) u_n(\vec{r}) = E_n u_n(\vec{r}). \tag{9}$$

Consider the boundary value problem of the following type:

$$\left[\frac{1}{2m}\left(\vec{p} - \frac{q}{c}\vec{\nabla}\chi(\vec{r},t)\right)^2 + U(\vec{r})\right]\psi_n(\vec{r},t) = E_n\psi_n(\vec{r},t), \tag{10}$$

where $\chi(\vec{r},t)$ is an arbitrary function of the space–time coordinates. If the boundary conditions for the problems (9) and (10) coincide at $\chi \to 0$, the eigenfunctions of the problem (10) are defined by

$$\psi_n(\vec{r},t) = u_n(\vec{r}) \exp\left(i\frac{q}{\hbar c}\chi(\vec{r},t)\right), \tag{11}$$

where $u_n(r)$ is the eigenfunction of the problem (9) associated with the eigenvalue E_n.

Indeed, substituting solution (11) into Eq (10), we get Eq. (9).

Symmetrical properties of the Hamiltonian of Eq. (10) depend on the spatial profile of the function $\chi(\vec{r},t)$ and, as follows, symmetrical properties of wave functions (11) differ from symmetrical properties of free-atom wave functions. Eigenfunctions of boundary value problems (9) and (10) constitute the two complete orthonormal basis

$$\int u_n^*(\vec{r})\, u_m(\vec{r})\, dV = \delta_{nm}, \qquad \int \psi_n^*(\vec{r},t)\, \psi_m(\vec{r},t)\, dV = \delta_{nm}.$$

Hence any eigenfunction of boundary problem (10) may be represented as an expansion into a series of the free-atom eigenfunction and vice versa

$$\psi_n(\vec{r},t) = \sum_m C_{nm}(t)\, u_m(\vec{r}), \tag{12}$$

$$u_n(\vec{r}) = \sum_m D_{nm}(t)\, \psi_m(\vec{r},t), \tag{13}$$

where expansion coefficients are defined by the following expressions:

$$\begin{aligned} C_{nm}(t) &= \int u_m^*(\vec{r}) \exp\left(i\frac{q}{\hbar c}\chi(\vec{r},t)\right) u_n(\vec{r})\, dV, \\ D_{nm}(t) = \int \psi_m^*(\vec{r},t)\, u_n(\vec{r})\, dV &= \int u_m^*(\vec{r}) \exp\left(-i\frac{q}{\hbar c}\chi(\vec{r},t)\right) u_n(\vec{r})\, dV. \end{aligned}$$

Substituting (12) into (13), one arrives at

$$\sum_m C_{nm} D_{mp} = \delta_{np}. \tag{14}$$

It is convenient to put into operation the Hermitian transformation matrix

$$V_{nm}(t) = \int u_n^*(\vec{r}) \exp\left(-i\frac{q}{\hbar c}\chi(\vec{r},t)\right) u_m(\vec{r})\, dV. \tag{15}$$

In this case, condition (14) reads as the unitarity condition for the matrixes (15), i.e.,

$$V^+ = V^{-1}, \quad \text{or} \quad \sum_m V_{pm} V_{mn}^{-1} = \delta_{np}.$$

Notice that we have used the notation $V_{nm}^{-1} = \left(V^{-1}\right)_{nm}$.

Let us assume that $\chi(\vec{r},t)$ is given by

$$\chi(\vec{r},t) = \vec{A}(t)\,\vec{r}.$$

In this case, the Hamiltonian of the boundary problem (10) takes the form

$$H = \frac{1}{2m}\left(\vec{p} - \frac{q}{c}\vec{A}(t)\right)^2 + U(r). \tag{16}$$

It can be easily seen that Hamiltonian (16) coincides with the Hamiltonian of Eq. (7) in the long-wave approximation (LWA).

The eigenfunctions of the boundary value problem (10) for an atom in the field (10) now read

$$\psi_n(\vec{r},t) = u_n(\vec{r}) \exp\left(i\frac{q}{\hbar c}\vec{A}(t)\,\vec{r}\right). \tag{17}$$

Now we make an important remark.

The quantum number n in the case of the free-atom eigenvalue problem is really a set of three quantum numbers $n = \{n_r, l, m\}$, which are the radial quantum number, angular momentum, and its projection. It is seen that eigenvalues of problems (9) and (10) coincide exactly, but eigenfunctions are drastically different. The reason consists in the fact that the angular momentum is a conservative variable in the case of a free atom, but it is not a conservative variable in the case of an atom interacting with the laser field. Indeed, the angular momentum operator $\vec{l}$ does not commute with the Hamiltonian (16). We have used the same type of indices to mark the states of problems (9) and (10). However, we should note that the index n in (17) means only that the energy of this state coincides with the energy of the nth free-atom state in the limit of $\left|\vec{A}\right| \to 0$. Indeed, the eigenfunctions of the free-atom states corresponding

to the zero angular momentum (nS states in atomic notations) do not depend on the angular variables. On the other hand, the wave function $\psi_{ns}(\vec{r},t)$ is

$$\psi_{ns}(\vec{r},t) = 4\pi u_{ns}(r) \sum_{l=0}^{\infty} \sum_{m=-l}^{l} i^l j_l\left(\frac{qA(t)\,r}{\hbar c}\right) Y_{lm}^*\left(\frac{\vec{A}}{A}\right) Y_{lm}\left(\frac{\vec{r}}{r}\right).$$

It is seen that the wave function of such a state is the infinite superposition of spherical functions with various l. Such kind of particle-wave-function transformation in the presence of a laser field can be easily predicted with the help of the classical model discussed in Sec. 1. Indeed, the state of the electron in the atom is characterized by the direction and magnitude of angular momentum. The magnitude of angular momentum is defined by the quantization rule (3). The radius of the orbital motion determines the particle energy. In a weak laser field, the electron angular momentum precesses around the laser-field direction, but its magnitude remains invariable. Along with the orbital motion, the electron makes a quiver motion in the laser-field direction. The electron energy averaged over the period of the optical oscillations remains invariable, and it changes only when the electron makes jumps between different atomic steady states.

The efficiency of the axially symmetric eigenfunctions (17) as a basis for the wave-function expansion can be illustrated in the following way.

The wave functions (17) are exact solutions of the right-hand side of Eq. (7). Hence for the matrix elements of the Hamiltonian for this equation we get

$$\int \psi_n^* H \psi_m \, dV = E_n \delta_{nm}.$$

On the other hand, matrix elements of this Hamiltonian with free-atom eigenfunctions are

$$\int u_n^* H u_m \, dV = \sum_p V_{np}^{-1}(t)\, E_p V_{pm}(t). \tag{18}$$

So these matrix elements are infinite sums. At the same time, it is very convenient to use free-atom eigenfunctions as a basis for the wave-function expansion, because the atom possesses its own eigenstates before and after interaction with the laser pulse. Of crucial importance is the fact that the matrix elements $V_{nm}(t)$ defined by (15) can be calculated in the exact analytical form. These matrix elements depend on the laser-pulse parameters (field amplitude, carrier frequency, temporal width, etc.) Hence, the number of summands providing a significant contribution to the right-hand side of (18) at given laser-pulse parameters can be determined before we start the numerical calculations with the equations for the probability amplitudes.

In view of Eq. (18), we obtain two equations for the probability amplitudes:

$$\begin{aligned} i\frac{da(k,l,t)}{\mathrm{d}t} &= \sum_{n,\lambda''}\sum_{m,l',\lambda'} V_{km}^{-1(l,\lambda')}\omega_{m,\lambda'}V_{mn}^{(\lambda',\lambda'')}a_{n,\lambda''}(t)+s \\ &+\sum_{m,\lambda'}\sum_{l'}\int d\mu\; V_{km}^{-1(l,\lambda')}\omega_{m,\lambda'}V_{m\mu}^{(\lambda',l')}a\left(\mu,l',t\right) \\ &+\sum_{n,\lambda'',l'}\int d\mu\; V_{k\mu}^{-1(l,l')}\frac{\hbar}{2m}\mu^2V_{\mu n}^{(l',\lambda'')}a_{n,\lambda''}(t) \\ &+\sum_{l'',l'}\int d\mu'\int d\mu\; V_{k\mu}^{-1(l,l')}\frac{\hbar}{2m}\mu^2V_{\mu n}^{(l',l'')}a\left(\mu',l'',t\right), \end{aligned} \tag{19}$$

and

$$\begin{aligned} i\frac{da_{n,l}(t)}{\mathrm{d}t} &= \sum_{p,\lambda''}\sum_{m,\lambda'} V_{nm}^{-1(l,\lambda')}\omega_{m,\lambda'}V_{mp}^{(\lambda',\lambda'')}a_{p,\lambda''}(t) \\ &+\sum_{m,\lambda'}\sum_{p,l',l''}\int d\mu\; V_{pm}^{-1(l',\lambda')}\omega_{m,\lambda'}V_{m\mu}^{(\lambda',l'')}a\left(\mu,l'',t\right) \\ &+\sum_{m,\lambda',l'}\int d\mu\; V_{n\mu}^{-1(l,l')}\frac{\hbar}{2m}\mu^2V_{\mu m}^{(l',\lambda')}a_{m,\lambda'}(t) \\ &+\sum_{l'',l'}\int d\mu'\int d\mu\; V_{n\mu}^{-1(l,l')}\frac{\hbar}{2m}\mu^2V_{\mu n}^{(l',l'')}a\left(\mu',l'',t\right). \end{aligned} \tag{20}$$

To characterize the dependence of matrix elements V_{nm} on the field amplitude, it is convenient to introduce the following parameter:

$$\varphi_0=\frac{eA_0a_B}{\hbar c}=\frac{eE_0a_B}{\hbar\omega_0}, \tag{21}$$

where a_B is the Bohr radius and E_0 is the laser-field amplitude. The parameter φ_0 can be represented as the ratio $\varphi_0=F_0/F_{at}$, where F_0 is the force acting on the electron from the laser field

$$F_0=qE_0=\frac{q\omega A_0}{c}$$

and F_{at} is the force acting on the electron from its parental nucleus

$$F_{at}=\frac{\partial U}{\partial r}\approx\frac{\hbar\omega}{a_B}.$$

There is a simple relationship between the well-known Keldysh parameter γ and parameter φ_0, namely, $\varphi_0=1/\gamma$.

3. Photoemission Spectra of a Single Atom

In the model of the point atom, the spectrum of the field of response (or emission spectrum) coincides with the spectrum of the atomic current density defined by

$$\vec{j}(r,t)=\frac{e}{m}\sum_{nm}\left(\vec{p_e}-\frac{e}{c}\vec{A}\left(r_e\right)\right)_{nm}a_n^*(t)a_m(t).$$

We obtain

$$\vec{j}_{nm} = \frac{q}{m}\int u_n^*(\vec{r})\left(\vec{p} - \frac{q}{c}\vec{A}\right)u_m(\vec{r})\ dV = \frac{q}{m}\sum_{k,p} V_{nk}^{-1}\vec{p}_{kp}V_{pm}$$

Solutions of the system of equations (19–20) provide necessary population-probability amplitudes but should be anticipated by study the associated matrix elements.

3.1. Matrix Elements for Transitions in Discrete and Continuum Bands

A number of general properties of the matrix elements V_{nm} can be directly derived from Eq. (15). Let us summarize some of them.

- The matrix elements of transitions between states of identical $V_{nm}^{(e)}$ and opposite $V_{nm}^{(o)}$ parity are defined by

$$V_{nm}^{(e)} = \int u_n^*(\vec{r})\cos\left(\frac{q}{\hbar c}\vec{A}(t)\,\vec{r}\right)u_m(\vec{r})\ dV, \qquad V_{nm}^{(o)} = -i\int u_n^*(\vec{r})\sin\left(\frac{q}{\hbar c}\vec{A}(t)\,\vec{r}\right)u_m(\vec{r})\ dV.$$

- Matrix elements $V_{nm}^{(e)}$ are the infinite series of even powers of field, and matrix elements $V_{nm}^{(o)}$ are the infinite series of odd powers of field.

- If the laser field amplitude tends to zero ($A \to 0$), the diagonal matrix elements ($n = m$) tend to unity, while the nondiagonal matrix elements ($n \neq m$) tend to zero.

With the help of eigenfunctions of the hydrogen spectra for the matrix elements between some low-laying states, we obtain

$$\langle 1s|\,V\,|1s\rangle = \frac{16}{(4+\varphi(t)^2)^2}, \qquad \langle 2s|\,V\,|2s\rangle = \frac{1-3\varphi(t)^2+2\varphi(t)^4}{(1+\varphi(t)^2)^4},$$

$$\langle 2p, m=1|\,V\,|2p, m=1\rangle = \frac{1}{(1+\varphi(t)^2)^3}, \qquad \langle 2p, m=0|\,V\,|2p, m=0\rangle = \frac{1-5\varphi(t)^2}{(1+\varphi(t)^2)^4},$$

$$\langle 1s|\,V\,|2s\rangle = \frac{256\sqrt{2}\varphi(t)^2}{(9+4\varphi(t)^2)^3}, \qquad \langle 1s|\,V\,|2p\rangle = \frac{384\sqrt{2}\varphi(t)}{(9+4\varphi(t)^2)^3}, \qquad \langle 2s|\,V\,|2p\rangle = \frac{3\varphi(t)\left(1-\varphi(t)^2\right)}{(1+\varphi(t)^2)^4},$$

where

$$\varphi(t) = \varphi_0 T(t).$$

It is seen that the matrix elements written above satisfy all properties mentioned above and also demonstrate some additional properties, which consist in the fact that the diagonal matrix elements sharply drop out when $\varphi_0 \approx 1$, and nondiagonal matrix elements achieve their maxima in the region of $\varphi_0 \approx 1$.

The matrix elements of ionization transitions can also be calculated in the analytic form with the help of hydrogen continuum spectrum eigenfunctions, which are

$$\Psi_k = \frac{C_{kl}}{(2l+1)!}(2kr)^l e^{-ikr} F\left(\frac{i}{k}+l+1, 2l+2, 2ikr\right)Y_l(\theta) = R_{kl}(r)Y_l(\theta),$$

where

$$C_{kl} = 2ke^{\pi/2k}\left|\Gamma\left(l+1-\frac{i}{k}\right)\right|,$$

$F\left(\frac{i}{k}+l+1,\, 2l+2,\, 2ikr\right)$ is the confluent hypergeometric function, $\Gamma\left(l+1-i/k\right)$ is the Gamma function, and $Y_l\left(\theta\right)$ is the spherical function. Notice, that in the above equations the wave number k is dimensionless due to its multiplication with the Bohr radius a_B.

The states of the continuum spectrum are infinitely degenerated with respect to the angular momentum. Due to the dipole approximation selection rules $\Delta l = \pm 1$, this degeneracy is not important in weak laser fields. However, at the near-atomic laser field strength, such structure of the continuum spectrum states affects crucially the emission spectra and angular distributions of the ionized electrons, because the spherical symmetry of the intra-atomic field is significantly broken by the laser field; as a result, the dipole approximation selection rules cease to be valid.

We have calculated the matrix elements $V_{k1s}^{(l)}$ for l running from 0 to 5. For example, in the case of $l = 1$ the matrix element is

$$V_{1s\to k} = \langle 1s|l=1\rangle = \frac{2k^2\sqrt{\pi}e^{\pi/2k}\left|\Gamma\left(2-i/k\right)\right|}{\sqrt{3}}$$
$$\times\left\{\frac{\Gamma(3)}{\varphi(t)}\left[\frac{{}_2F_1\left(\frac{i}{k}+2,3;4;\frac{2ik}{ik+1-i\varphi(t)}\right)}{\left(ik+1-i\varphi(t)\right)^3}+\frac{{}_2F_1\left(\frac{i}{k}+2,3;4;\frac{2ik}{ik+1+i\varphi(t)}\right)}{\left(ik+1+i\varphi(t)\right)^3}\right]\right.$$
$$\left.-\frac{\Gamma(2)}{\left(\varphi(t)\right)^2 i}\left[\frac{{}_2F_1\left(\frac{i}{k}+2,2;4;\frac{2ik}{ik+1-i\varphi(t)}\right)}{\left(ik+1-i\varphi(t)\right)^2}-\frac{{}_2F_1\left(\frac{i}{k}+2,2;4;\frac{2ik}{ik+1+i\varphi(t)}\right)}{\left(ik+1+i\varphi(t)\right)^2}\right]\right\},$$

where ${}_2F_1$ is the hypergeometric function and $T(t)$ is the temporal profile of the laser field. Other matrix elements have the similar form.

When the laser-field strength exceeds the intra-atomic field level, the atomic response could be consistently described only if we take into account the fact that the ionized electron wave function is the sum over continuum spectrum eigenfunctions with different angular momenta. The input of each angular momentum state is directly determined by the magnitude of an appropriate matrix element $V_{1s\to k}^{l}$.

3.2. Analytically and Numerically Calculated Emission Spectra

The quantity of matrix elements needed for "exact" solving of the set of equations (19)–(20) consists of an infinite number of equations. However, the calculated matrix elements enable one to estimate the required number of equations at any given parameters of the laser pulse (amplitude, frequency, temporal width). The results of the numerical and analytic calculations of emission spectra are presented in Figs. 1 and 2. Figure 2 shows the emission spectrum of a hydrogen-like atom in the ground 1s state. The two curves in this figure correspond to the cases where two and five terms have been taken into account in expansion (12). It is clearly seen that the matrix elements with the highest value give the main input. The profile of the spectrum is practically unchanged if we take into account the additional terms.

This allows us to state that, in the case of an initially non-excited atom driven by the near-atomic external field, the main contribution to processes of HHG and ionization give the ground state and

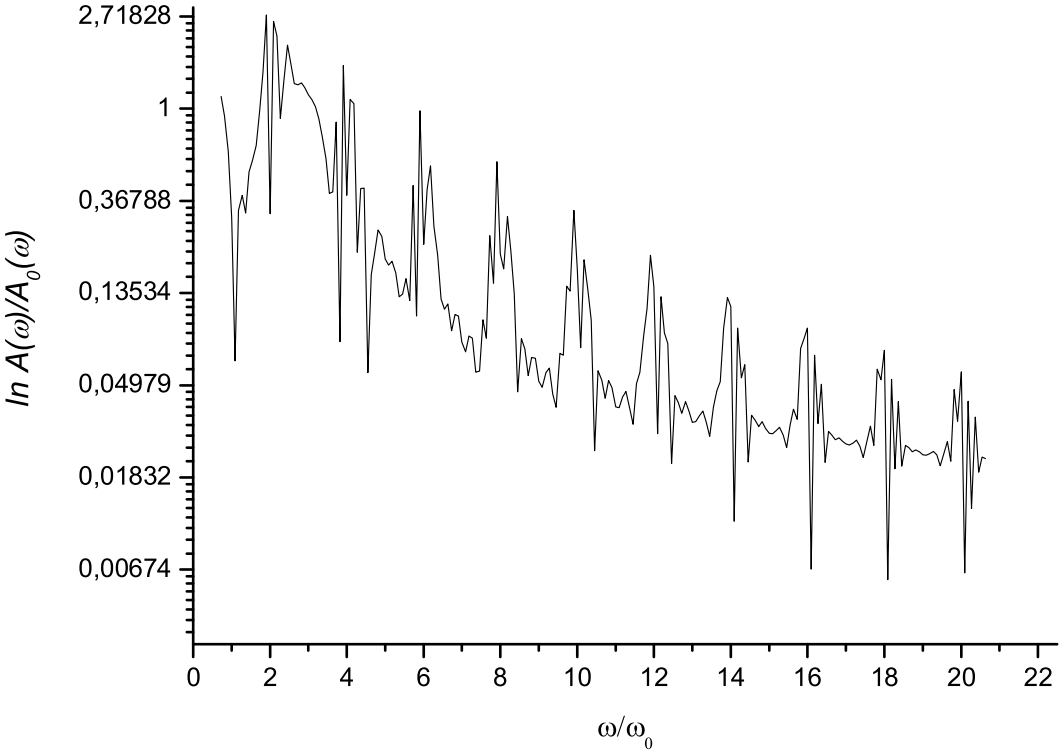

Fig. 1. Emission spectra of a single hydrogen-like atom (1s-2p-3s) driven by laser pulse with the electric-field amplitude $E = 1.3\,E_{\rm at}$ (numerical calculation).

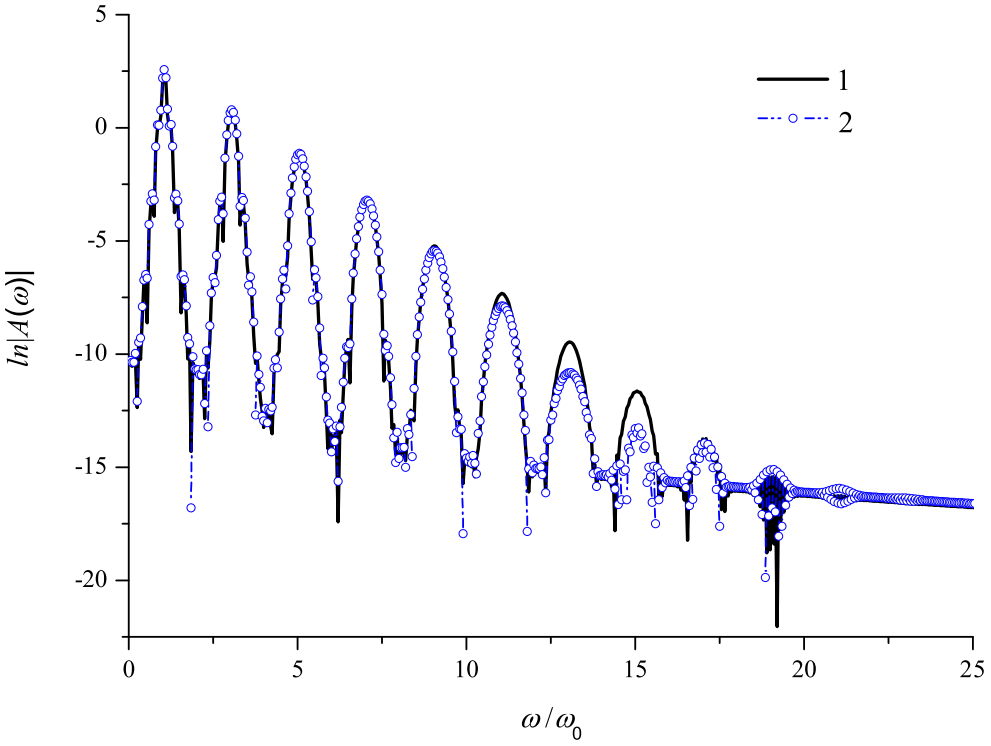

Fig. 2. Emission spectra of a single hydrogen-like atom (1s-2p-1s), curve 1, and (1s-2p-2s-3s-3p-3d), curve 2, driven by a laser pulse with the electric field amplitude $E = E_{\rm at}$ (analytical calculation)

some low states located nearby. The reason for the small contribution of exited states consists in their instability under the external-field impact.

4. Angular Distributions of the Ionized Electrons

The results below deal with involvement of continuum band wave functions and, as follows, ionization processes. Modification of the selection rules could be fairly seen on the angular distribution of ionized electrons.

4.1. Selection Rules for Orbital Quantum Numbers

Let us turn now to a detail discussion of the dependences of the ionization transition matrix elements presented in Fig. 3. The laser field strength varies in the region from $0.005E_{\text{at}}$ up to $2.5E_{\text{at}}$.

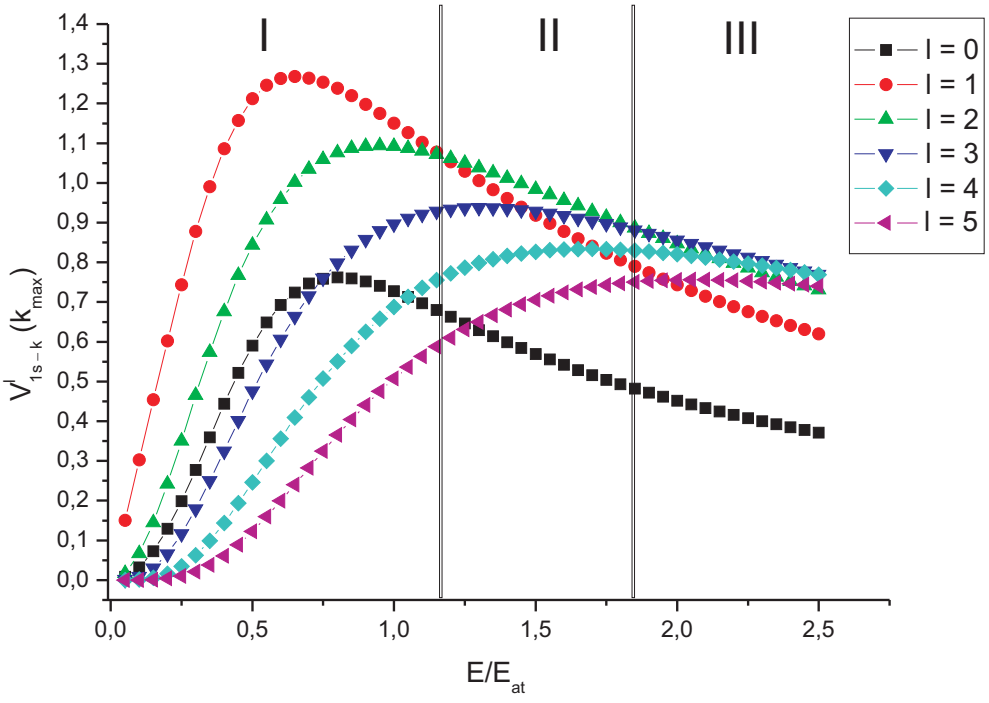

Fig. 3. Maximum value of ATI matrix elements as a function of the laser-field amplitude normalized to the intra-atomic field strength. Angular momentum l runs from 0 to 5.

The first region in Fig. 3 corresponds to the conditions under which the eigenstates of $l = 1$ dominate over any other states in the wave function of the ionized electron. In this region of the laser-field strength, the atomic response agrees reasonably well with the dipole approximation selection rules, i.e., $\Delta l = \pm 1$. On the other hand, when the laser-field strength exceeds the intra-atomic field strength, the probability of transitions to the continuum states of $l = 2$ exceeds that for $l = 1$, as is clearly seen in Fig. 3. Hence, in the second region, the atomic response ceases to be completely determined by the dipole-approximation selection rules. It is also seen, that in the region of the over-atomic laser field strength the atomic

response could not be reasonably calculated without taking into account the ionized electron states with high angular momentum, i.e., $l > 1$.

4.2. Angular Distribution Features

In the regime of the above-threshold ionization (ATI), the laser photon energy exceeds the ionization energy. In this case, the set of equations (19)–(20) can be substantially simplified, because from the variety of the discrete spectrum states only the ground state has the nonzero probability to be populated and, hence, only this state of the discrete spectrum should be taken into account. The matrix elements of V were calculated above for discrete-discrete $\langle d|V|d'\rangle$ and discrete-continuum $\langle d|V|c\rangle$ transitions. It can easily be shown that the magnitude of these matrix elements exceeds significantly the magnitude of matrix elements for the continuum–continuum transitions $\langle c|V|c'\rangle$. As a result, the sums $\sum\limits_m V_{nm}E_mV^{-1}_{mk}$ include the summation over the discrete-spectrum states only. Thus, in the case of the ATI process, the set of equations (19)–(20) reads

$$\frac{\mathrm{d}a_{il}(t)}{\mathrm{d}t} = -iE\left(y_i(t,l)b(t) + \sum_{m=0}^{l_{\max}}\sum_{k=0}^{n_{\max}} d_{ik}(t,l,m)a_{km}(t)\right), \tag{22}$$

$$\frac{\mathrm{d}b(t)}{\mathrm{d}t} = -i\left[\left(V_{1s1s}V^{-1}_{1s1s} - \sum_{l=0}^{l_{\max}}\sum_{k=1}^{n_{\max}} V^{(l)}_{1s\to k}k^2V^{-1(l)}_{1s\to k}\right)b(t) + E\sum_{l=0}^{l_{\max}}\sum_{k=1}^{n_{\max}} {y_k}^*(t,l)a_{kl}(t)\right], \tag{23}$$

where $a_i(t)$ are the probability amplitudes for continuum states, $b(t)$ is the probability amplitude for the ground state, and

$$y_i(t,l) = V_{1s1s}V^{-1(l)}_{1s\to i}, \qquad d_{ik}(t,l,m) = V^{(l)}_{i\to 1s}V^{-1(m)}_{1s\to k}.$$

The solution of the above equations provides the spatial profile of the wave function of the ionized electrons

$$\psi_{\mathrm{photoel}}(\vec{r},t) = \int dk\ a(k,l,t)u(k,l,\vec{r}).$$

The angular distributions of the ionized electrons are given by the Fourier transform of the wave function

$$\begin{aligned}\psi_{\mathrm{photoel}}(\vec{k},t) = {} & \sqrt{4\pi}\sum_{l=0}^{5}\sum_{n=0}^{n_{\max}} a(n,l,t)i^{2l}\sqrt{2l+1}(2(n-i\delta)^2)^l\,\frac{\exp\left[\pi/2(n-i\delta)\right]\left|\Gamma\Big(l+1-i/(n-i\delta)\Big)\right|}{k(2l+1)!}\\
& \times\Bigg(\sum_{j=0}^{l}\frac{i^{-l+j-1}(l+j)!}{j!(l-j)!(2k)^j}\Gamma\left(l-j+2\right)\left(i((n-i\delta)-k)\right)^{(-(l-j+2))}\\
& \times{}_2F_1\left(\frac{i}{n-i\delta}+l+1, l-j+2; 2l+2; \frac{2(n-i\delta)}{n-i\delta-k}\right)\\
& +\sum_{j=0}^{l}\frac{i^{-l+j-1}(l+j)!}{j!(l-j)!(2k)^j}\Gamma\left(l-j+2\right)\left[i((n-i\delta)+k)\right]^{(-(l-j+2))}\\
& \times{}_2F_1\left(\frac{i}{n-i\delta}+l+1, l-j+2; 2l+2; \frac{2(n-i\delta)}{n-i\delta+k}\right)\Bigg)P_l(\cos\theta),\end{aligned} \tag{24}$$

where δ is the lifetime of the continuum state. In numerical calculations, we put $\delta = 0.27\,\omega_0^{-1}$. It is seen that the angular distributions are sums of the Legendre polynomials $P_l(\cos\theta)$, where θ is the angle between the photoelectron wave vector $\vec{k}$ and the vector potential $\vec{A}$ of the laser field.

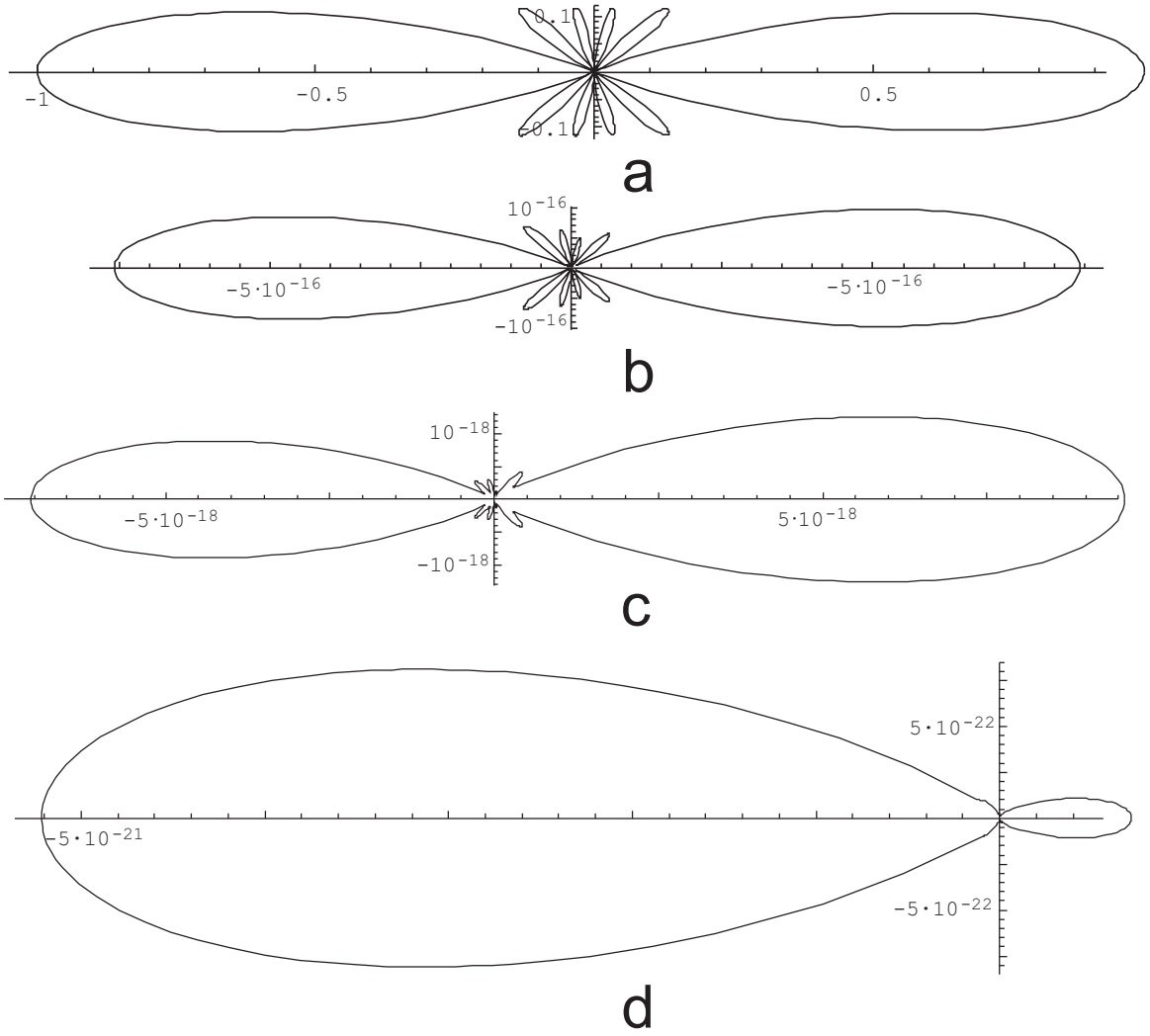

Fig. 4. Angular distributions of photoelectrons with $k = 0.05$ (a), 0.95 (b), 1.55 (c), and 4.25 (d) at the external field amplitude $E = 2.5E_{\rm at}$.

Angular distributions of ionized electrons (a sample from the number of them) are shown in Fig. 4. At the near-atomic laser filed strength, we can clearly see the appearance of the additional wings. Within the framework of the perturbation theory, the spectrum of ionized electrons is a comb of maxima $E = E_0 + n\hbar\omega$. According to the dipole approximation, the electron transitions from the state of angular momentum l to the states of $l \pm 1$ have approximately the same probability. As a result, for the angular distributions of the ionized electrons of energy $E = E_0 + n\hbar\omega$, we obtain

$$p_n(\theta) \sim \left| \sum_{l=\{l_0-n,\,0\}}^{l_0+n} a_l P_l(\cos\theta) \right|^2 ,$$

where l_0 is the angular momentum of the ground atomic state. It is seen that the angular distributions presented in Fig. 4 cannot be described by this equation. The angular distributions depend significantly on the ionized electron energy $E = \hbar^2 k^2/2m$, but the increase in the electron energy is not accompanied by an increase in the number of side lobs. Such behavior of the angular distributions is in qualitative agreement with the results of the experimental measurements by Nandor et al. [8]. An additional feature of the samples is that the angular distributions are asymmetric with respect to directions $\theta = 0^\circ$ and $\theta = 180^\circ$. This is due to the finite temporal width of the laser pulse.

We should note that in the subatomic region of the laser field strength, angular distributions that arise in our numerical experiments are reasonably well modeled by a Legendre polynomial of the first order. Angular distributions of such a kind are in agreement with the dipole selection rules.

5. Summary and Conclusions

The interaction of a single hydrogen-like atom with the laser pulse of the near-atomic field strength has been studied. The presented theory is based on the use of the exact solutions of the eigenvalue problem on the particle motion in a cylindrically symmetric field (CSF) as a basis for the wave-function expansion. The superposition of the spherically symmetric intra-atomic field and linearly polarized laser field has the cylindrical symmetry. Hence, the use of the free-atom eigenfunctions as a basis for the wave-function expansion requires an infinitely increasing number of spherical harmonics (i.e., free-atom eigenfunctions) when the laser field strength approaches the intra-atomic field strength. The CSF problem eigenfunctions directly depend on the laser field strength. As a result, they do not require imposing limitation on the ratio of the laser field strength to the intra-atomic field strength $E_0/E_{\rm at}$, and the calculated matrix elements are nonlinear functions of the field strength. Thus the contribution of any nonlinear process to the atomic emission spectra is taken into account in a consecutive manner.

In the region of subatomic field strength, the spectra calculated are in agreement with the classical picture of the odd harmonic train with the cut-off frequency linearly depending on the laser field intensity. In the region of the near-atomic field strength, the emission spectra take the form of the quasicontinuum generation spectra. Nevertheless, they display the plateau and cut-off frequency. As the laser field strength approaches the intra-atomic field strength, the cut-off frequency rises as the laser-pulse intensity slows down and then it saturates.

In the region of the near-atomic field strength, the energy spectrum of the ionized electrons is a wide curve with one peak at $E_0 < E_{\rm at}$ and a few peaks at $E_0 > E_{\rm at}$. The appearance of the additional maxima is due to the increase of the contribution of the high l continuum states. Angular distributions of the ionized electrons have been calculated. At the near-atomic laser field strength, the angular distributions are significantly different from that calculated with the help of the perturbation theory. They show clearly that the probability of ionization transitions to the continuum states of different l depends substantially on the energy of the ionized electron. The results obtained are in agreement with the recent experimental data.

Acknowledgments

This work was partially supported by the Russian Foundation for Basic Research under Project No. 08-02-16764.

References

1. W. Becker, F. Grasbon, R. Kopold, et al., *Advances in Atomic, Molecular, and Optical Physics*, Elsevier, **48**, 35 (2002).
2. A. V. Andreev, *J. Exp. Theor. Phys.*, **116**, 793 (1999).
3. K. C. Kulander and B. W. Shore, *Phys. Rev. Lett.*, **62**, 524 (1989).
4. G. Bandarage, A. Maquet, and J. Cooper, *Phys. Rev. A*, **41**, 1744 (1990).
5. R. A. Sacks and A. Szoke, **Phys. Rev. A**, **40**, 5614 (1989).
6. R. M. Potvliege and R. Shakeshaft, *Phys. Rev. A*, **40**, 3061 (1989).
7. R. A. Ganeev, M. Baba, M. Suzuki, and H. Kuroda, *Phys. Lett. A*, **339**, 103 (2005).
8. M. J. Nandor, M. A. Walker, and L. D. Woerkom, *J. Phys. B.: At. Mol. Opt. Phys.*, **31**, 4617 (1998).
9. A. V. Andreev and O. A. Shoutova, *Phys. Lett. A*, **350**, 309 (2006).
10. A. V. Andreev, O. A. Shoutova, and S. Yu. Sremoukhov, *Laser Phys.*, **17**, 496 (2007).
11. L. D. Landau and E. M. Lifshits, *Quantum Mechanics*, 3rd ed., Elsevier Science, Saint Louis (1981).
12. Ba Lihua, Jingtao Zhang, Zhizhan Xu, and Dong-Sheng Guo, *Phys. Rev. Lett.*, **97**, 193004 (2006).
13. H. M. Nilsen, L. B. Madsen, and J. P. Hansen, *J. Phys. B: At. Mol. Opt. Phys.*, **35**, 403 (2002).